J. Biophotonics **10**, No. 2, 224–230 (2017) / **DOI** 10.1002/jbio.201500208

Journal of BIOPHOTONICS

FULL ARTICLE

Bare fiber Bragg grating immunosensor for real-time detection of *Escherichia coli* bacteria

Rajesh Srinivasan[1], *Sharath Umesh*[2], *Swetha Murali*[1], *Sundarrajan Asokan*[2, 3], *and Sai Siva Gorthi*[*, 1]

[1] Optics & Microfluidics Instrumentation Lab, Department of Instrumentation and Applied Physics, Indian Institute of Science, Bangalore-560012, India
[2] Department of Instrumentation and Applied Physics, Indian Institute of Science, Bangalore-560012, India
[3] Applied Photonics Initiative and Robert Bosch Centre for Cyber Physical Systems, Indian Institute of Science, Bangalore-560012, India

Received 6 August 2015, revised 12 December 2015, accepted 18 December 2015
Published online 12 January 2016

Key words: biosensors, fiber optic technology, quality control, immunoassay, pathogenesis

Escherichia coli (*E. coli*) bacteria have been identified to be the cause of variety of health outbreaks resulting from contamination of food and water. Timely and rapid detection of the bacteria is thus crucial to maintain desired quality of food products and water resources. A novel methodology proposed in this paper demonstrates for the first time, the feasibility of employing a bare fiber Bragg grating (bFBG) sensor for detection of *E. coli* bacteria. The sensor was fabricated in a photo-sensitive optical fiber (4.2 μm/80 μm). Anti-*E. coli* antibody was immobilized on the sensor surface to enable the capture of target cells/bacteria present in the sample solution. Strain induced on the sensor surface as a result of antibody immobilization and subsequent binding of *E. coli* bacteria resulted in unique wavelength shifts in the respective recording of the reflected Bragg wavelength, which can be exploited for the application of biosensing. Functionalization and antibody binding on to the fiber surface was cross validated by the color development resulting from the reaction of an appropriate substrate solution with the enzyme label conjugated to the anti-*E. coli* antibody. Scanning electron microscope image of the fiber, further verified the *E. coli* cells bound to the antibody immobilized sensor surface.

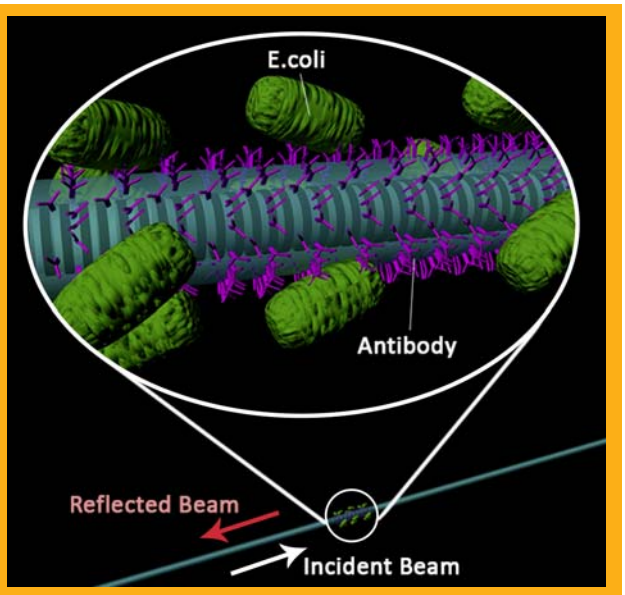

* Corresponding author: e-mail: saisiva.gorthi@iap.iisc.ernet.in

1. Introduction

Infections owing to the consumption of food and water contaminated with *E. coli* bacteria are correlated with the pathogenesis of several diseases [1]. Toxins released by certain *E. coli* types can damage the epithelial cells in the intestine, result in bladder infections, lead to diarrhea and damage kidneys [2]. Periodic inspection of samples to identify *E. coli* bacteria can provide a reasonable evidence of fecal contaminants and presence of other pathogenic bacteria [3]. This information is vital to limit the extent of the resultant disease outbreaks and to provide valuable guidelines to the regulatory bodies to take timely measures. Different methods have been explored for the identification of *E. coli* bacteria from a variety of samples. Earliest method of detection involves manual counting of the viable bacterial colonies once they are grown in selective nutrient-rich media for a span of 1–2 days. With the advent of techniques like Polymerase chain reaction (PCR) [4] and Enzyme linked immunosorbent assay (ELISA) [5], the time for test has been reduced considerably. As of today, ELISA is the gold standard technique for *E.coli* detection. It employs enzyme linked antibodies against the whole *E. coli* cell or its surface proteins, for their detection. The main drawback with this technique is that it cannot be used for real-time identification of *E. coli*. Thus, for rapid and real-time detection of *E. coli* and other bacteria present in a given sample, there has been considerable research interest in developing highly sensitive, easy to use and cost effective biosensors.

Of the different transduction methods reported in literature for biosensors [6, 7], optical methods offer the benefits of higher sensitivity, faster response and greater immunity to ambient electromagnetic noise. Amongst the optical methods (biophotonic sensors), fiber based sensors are of particular interest, due to their ease-of-implementation. Earliest fiber optic biosensors employed fluorescence based detection using labeled antibodies or target molecules [8]. In an effort to reduce the overall cost and process complexity, label-free methods capable of detecting refractive index changes (with target binding) were developed. Some of the notable methods employed the use of fiber tapers, surface plasmon resonance (SPR) and fiber couplers [9, 10].

A major advancement in the field of label-free optical biosensors is the advent of optical fiber gratings. Different types of optical grating sensors, Etched fiber Bragg grating (EFBG), Long period grating (LPG) and Tilted fiber Bragg grating (TFBG), have been employed for detection of biomolecules [11–13]. EFBG, LPG and TFBG differ from a bare fiber Bragg grating (bFBG) sensor in their effective cladding thickness, grating period and relative orientation of the grating respectively [14]. This difference in the grating properties in EFBG, LPG and TFBG enables them to interact with their surroundings which is exploited in biosensing. A number of works that employ LPG based sensors for *E. coli* detection have been reported [15–17]. The refractive index variation associated with the binding of target cell on the sensor surface, manifests as change in resonance condition for the grating structure. This in turn results in a continuous shift in the resonance peaks in the reflected/transmission spectrum, which is monitored. LPGs exhibit relatively lower refractive index sensitivity associated with the binding of bio-molecules in aqueous medium. To circumvent this problem and to achieve better sensitivity, LPGs are often deposited with high refractive index overlays [18]; thereby, complicating the fabrication process. On the other hand, the refractive index sensitivity of EFBG sensors have known to increase with increased etching of the cladding layer [11]. However, etching more of the cladding layer would increase fragility of the sensor.

In contrast to existing Bragg grating sensors adopted so far for biosensing, use of a bFBG represents a simpler paradigm owing to its sensing architecture and relative ease of fabrication. In this paper, we propose an antibody immobilized bFBG sensor for label-free detection of *E. coli* bacteria. The methodology adopted for sensing was demonstrated with *E. coli* K12 bacteria, which are non-pathogenic. However, the same can be extended for detection of other pathogenic varieties of bacteria. Covalent binding chemistry was adopted for attaching antibody on to the sensor surface. The reflected Bragg wavelength from the sensor at different stages of the experiment was recorded using the Micron Optics Fiber Bragg grating (FBG) interrogator. The interrogator used here acts as the source of incident light, as well as the data acquisition system for continous monitoring of interactions of the bFBG sensor with different reagents in real-time. Subsequent sections in this paper outline the protocols for functionalization of the bFBG sensor, experimental methodology adopted and also, discuss the resultant outcomes in terms of Bragg wavelength shift observed with antibody and *E. coli* binding on to the sensor surface.

2. Material and methods

2.1 FBG sensor theory

FBG is a refractive index modulation of the core introduced along the axis of a single mode photosensitive fiber by exposure to an intensity modulated UV light [19]. FBG reflects back a single wavelength that

satisfies the Bragg's resonance condition and transmits the remaining components of the spectrum, when a broad band light is launched into it [20]. The reflected Bragg wavelength is given by,

$$\lambda_b = 2 \cdot n_{\text{eff}} \cdot \Lambda \tag{1}$$

where n_{eff} is the effective refractive index of the core and Λ is the grating pitch. As the cladding completely isolates the core from its surroundings, FBG is inherently insensitive to the surrounding refractive index variation [21]. External parameters such as strain, temperature etc. that can alter the grating pitch of FBG can be precisely sensed by interrogating the relative shift in the reflected Bragg wavelength [22–24]. The wavelength shift as a result of strain induced on a FBG is given by,

$$\Delta\lambda_b = \lambda_b \left\{ 1 - \frac{n_{\text{eff}}^2}{2} (P_{12} - \upsilon[P_{11} - P_{12}]) \right\} \cdot \varepsilon \tag{2}$$

where ν is the Poissons ratio, and ε is the axial strain change, P_{11} and P_{12} are coefficients of the stress-optic tensor [24]. While sensing the strain, it is important to compensate for the shift in the reflected Bragg wavelength due to the temperature variations. In the present work, the temperature effect on FBG was neglected as all recordings were taken in controlled conditions. Different techniques have been reported in literature for fabrication of FBG. In the present study, phase mask technique has been employed for fabrication of bFBG sensor [25, 26].

2.2 Validation of antibody used in experiment

Polyclonal antibody against *E. coli* bacteria (Abcam, ab31499) and Horseradish peroxidase (HRP)-conjugated polyclonal antibody against *E. coli* bacteria (Abcam, ab68450) were purchased. Since the antibodies purchased were prepared against the whole *E. coli* cell and its surface proteins, its ability to bind with the specific *E. coli* K12 bacteria have to be validated. For this purpose, standard sandwich ELISA experiments were carried out in microtiter plates with appropriate controls. The unconjugated capture antibody was prepared in 0.1 M sodium carbonate buffer at a dilution factor of 1 : 2000 and the enzyme (HRP) conjugated detection antibody was prepared in 10 mM phosphate buffered saline-tween (PBS-T) solution at a dilution factor of 1 : 200. Enzyme substrate tetramethylbenzidene (TMB, Sigma Aldrich) was added to all the wells and the respective color changes were observed. The results indicated that the antibodies were functional and could be used to capture *E. coli* K12 bacterial cells.

2.3 Experimental methodology

bFBG sensor of gauge length 3 mm was fabricated in photo-sensitive silica fiber (SM1500) of cladding diameter of 80 μm using a 248 nm UV Excimer Laser (pulse energy of 6 mJ at 100 Hz repetition rate). This bFBG facilitated a grating period of 530 nm and center wavelength of 1559 nm. The fiber was pre-stretched and both ends were taped to a cleaned glass slide, such that a spacing of 50 μm was maintained between the fiber and the glass slide.

The approximate position of the sensor in the fiber was marked on the glass slide. The fiber was then connected to the Micron Optics FBG interrogator (SM130-700, resolution of 1 pm). The interrogator facilitates peak wavelength detection technique for data acquisition and records the peak reflected Bragg wavelength from the sensor at any given point of time, as shown in the pictorial representation in Figure 1(a). An enlarged schematic of the bFBG sensor post antibody immobilization and *E. coli* binding (the relevant protocols will be discussed in Sections 2.4 and 2.5) is shown in Figure 1(b). The photograph of the experimental setup used is shown in Figure 2. Fixed Volume (300 μL) of (i) water, (ii) anti-*E. coli* antibody solution and, (iii) sample containing *E. coli* bacteria were sequentially pipetted

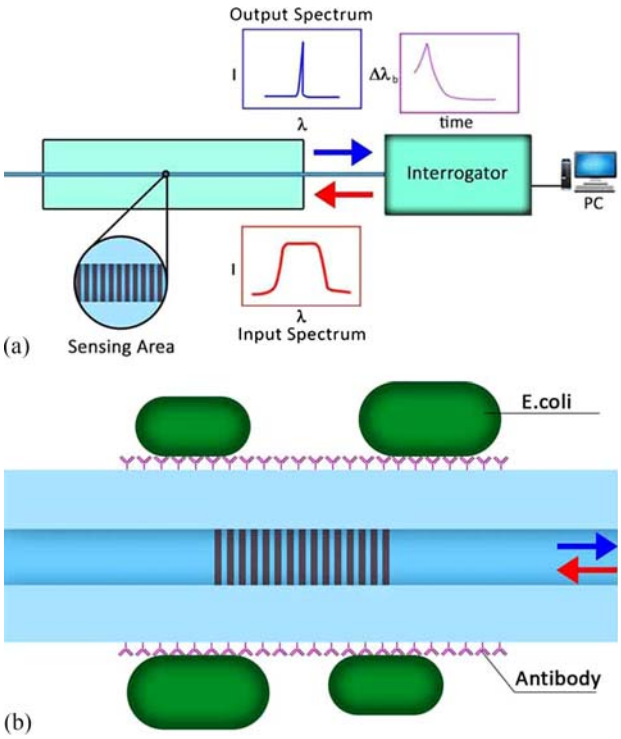

Figure 1 (**a**) Schematic of the experimental setup indicating the incident and the reflected light from the sensor. (**b**) Enlarged representation of the grating region after antibody immobilization and *E. coli* binding.

Figure 2 Photograph of the experimental setup.

onto the sensor surface after functionalization and the resultant temporal variations in the reflected Bragg wavelength were recorded in each case. Data was logged in before the respective samples were added and continuously recorded for subsequent 10 minutes. The experimental protocols adopted for functionalization of the sensor surface and for antibody immobilization are discussed in detail in the following sections.

2.4 Functionalization of the sensor surface

The protocol adopted here introduces reactive functional groups on the sensor surface for covalent binding with the amine side groups present in anti-*E. coli* antibody [27]. Sensor surface was cleaned by washing it sequentially with methanol- hydrochloric acid (1 : 1 v/v) solution, concentrated sulfuric acid, hot sodium hydroxide solution and boiling water, for 5 minutes each. Between each subsequent wash steps, the sensor was rinsed with deionized (DI) water. The sensor surface was then silanylated by incubating it with 5% aminopropyltriethoxysilane (APTES) solution (SigmaAldrich prepared in DI water at pH 3.0) for 15 minutes. The fiber was then washed with ethanol and dried, prior to baking at 80 °C for 30 minutes. Amine functionalized sensor surface was incubated in 1% glutaraldehyde solution (in DI water at pH 9.2) for 15 minutes to have sensor surface functionalized with aldehyde group.

2.5 Antibody immobilization and target cell binding

Aldehyde fuctionalized sensor surface was rinsed with 0.1 M carbonate-bicarbonate buffer (pH 9.2). Enzyme (HRP) conjugated anti-*E. coli* antibody was used in all experiments for ease of validation of binding to the sensor surface. Antibody solution diluted in 0.1 M carbonate buffer (300 µL, in 1 : 2000 ratio) was added over the functionalized sensor and incubated for 15 minutes. To block the non-specific sites, bovine serum albumin (BSA) 1% solution prepared in DI water (300 µL) was added and incubated for 10 minutes. The sensor was washed with phosphate buffered saline (PBS) solution. Subsequently, sample solution containing *E. coli* bacteria was added on to the sensor surface. After incubation for 15 minutes, the sensor was washed with DI water. The pictorial representation of the sensor after each step described in the experimental protocol is shown in Figure 3.

2.6 Cross-validation experiments

In order to validate the binding of antibody and *E. coli* bacteria, trial experiments were carried out on bare fibers that were used in the fabrication of bFBG sensors. Functionalized fiber was immersed in enzyme (HRP)-conjugated antibody solution prepared in carbonate buffer (dilution factor of 1 : 200)

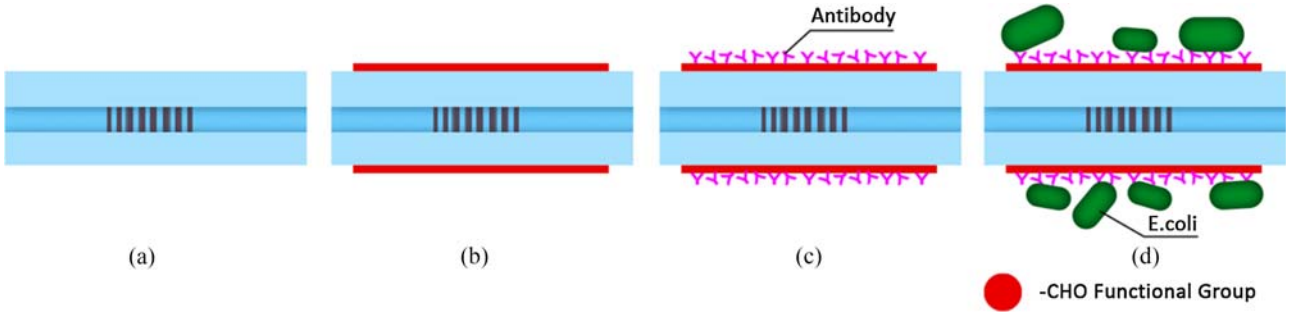

Figure 3 Schematic representation of (**a**) bFBG sensor, (**b**) bFBG sensor after functionalization, (**c**) sensor surface after anti-*E. coli* antibody immobilization, (**d**) sensor surface post *E. coli* binding.

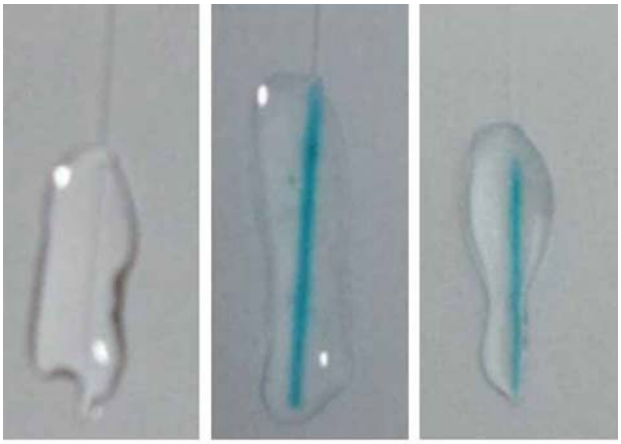

Figure 4 (**a**) Control fiber after substrate addition (**b**) Sample fiber after incubation with HRP-conjugated antibody and exposure to enzyme substrate (**c**) Sample fiber after antibody immobilization and PBS wash, re-exposed to enzyme substrate.

for 20 minutes. Substrate solution (TMB) was added on the fiber and the resultant color change was observed as shown in Figure 4(b). The fiber was then washed thoroughly with PBS buffer and was re-exposed to the substrate solution. The subsequent colour change indicated by the fiber after the PBS wash as shown in Figure 4(c), validated the binding of antibody on the fiber surface.

The fiber was then immersed in sample solution containing *E. coli* bacteria (1 : 100 dilution in DI water) for 30 minutes. Subsequently, it was rinsed with DI water and air dried before it was mounted

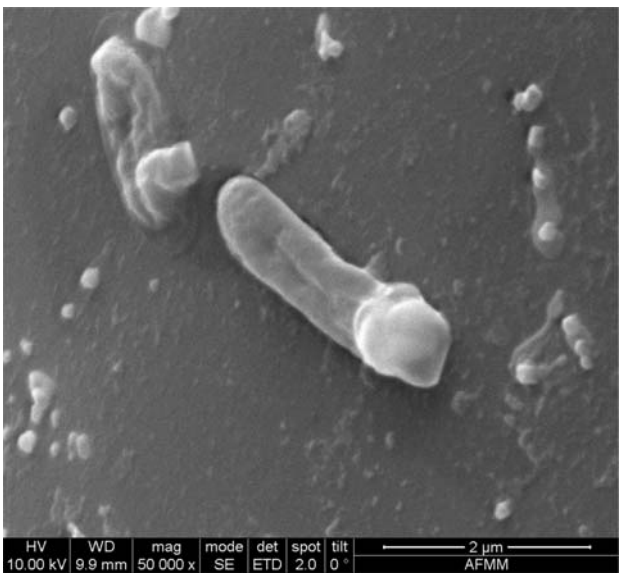

Figure 5 Scanning electron microscope (SEM) image of *E. coli* cells bound to the fiber surface.

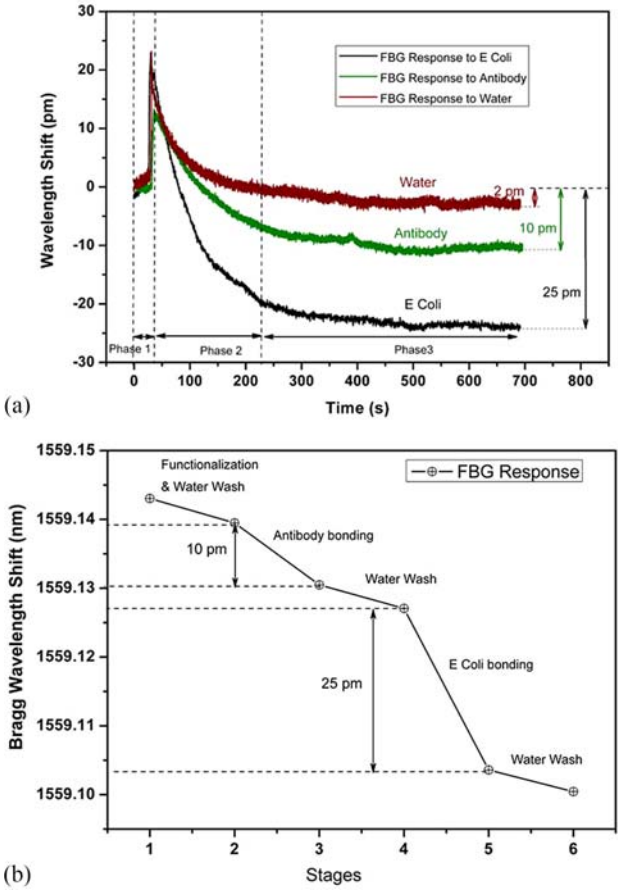

Figure 6 (**a**) Plot of wavelength shift vs time with different samples. (**b**) Plot of wavelength shift at the end of each stage of the experiment.

on the sample holder using a double sided carbon tape. For the purpose of validation, the sample was desiccated and later gold sputtered before images were taken using the scanning electron microscope (FEI ESEM Quanta 200).

Figure 5 shows the micrograph that was obtained indicating the *E. coli* cells bound to the fiber surface. In the actual experiments with the bFBG sensor, it was observed that the binding of antibody and *E. coli* bacteria happened within few minutes (10 minutes) and the interrogator recording served as the readout mechanism for real-time monitoring of *E. coli* cells bound to the sensor surface.

3. Results and discussions

Sensor responses on addition of different solutions were recorded using the interrogator. The reflected Bragg wavelength observed prior to the introduction of respective solutions, serves as the reference for

determining the wavelength shifts in the subsequent time intervals.

Phase 1: All three response curves in Figure 6(a) exhibited positive (red) shifts just after the respective samples were added over the sensor surface.

Phase 2: Data recorded subsequently, indicate a drop in wavelength shift. As water spreads out evenly on the sensor surface, it was observed that the reflected Bragg wavelength approach the reference value. However, in the other two cases, exponential drop in the response curves were followed by subsequent negative (blue) shifts resulting from the binding of antibody and *E. coli* bacteria on to the sensor surface.

Phase 3: The sensor responses approached an equilibrium condition in this phase. It was observed that the wavelength shift with water got normalised. The wavelength shift with antibody and *E. coli* solutions saturated at –10 pm and –25 pm respectively. It was inferred that these shifts were the result of the respective strain experienced by the sensor due to antibody and *E. coli* cells bound to the surface. The dimension and the net mass of *E. coli* is more than that of the antibody, which is evident from the higher wavelength shift observed with *E. coli* binding as compared to antibody attachment.

The plot of the reflected Bragg wavelength at the end of different stages of the experiment is as shown in Figure 6(b). From the response curves, it is evident that continuous observation of reflected Bragg wavelength can be used for monitoring the interaction of different samples with the bFBG sensor. Minimal amounts of shifts were observed during wash steps. Experiments were repeated with multiple bFBG sensors and the variation in the reflected Bragg wavelength shifts were recorded. Similar patterns in wavelength shift were observed with different sensors in subsequent trials. Current study demonstrated the potential of the bFBG to detect the binding of *E. coli* bacteria. The same study can be extended and the proposed bFBG sensor can be adopted for detection of a variety of disease specific biomarkers, bacteria, clinically relevant proteins and cells etc., after immobilizing the bFBG sensor surface with appropriate antibody. However in actual field trials, where variations in temperature will occur, a sacrificial FBG sensor will be employed to explicitly measure temperature variations. The effect of temperature variations over the bFBG for sensing can be negated using the data obtained from the FBG temperature sensor.

4. Conclusion

The applicability of an antibody immobilized bFBG sensor for detection of *E. coli* bacteria was demonstrated. By continuously acquiring the shift in the reflected Bragg wavelength, it was possible to dynamically monitor the interaction of *E. coli* bacteria with the sensor. Further, it was observed that the sensitivity of the proposed methodology was high enough to respond to the binding of anti-*E. coli* antibody, producing a shift in the reflected Bragg wavelength of the order of few picometers. Results obtained with the proposed methodology have been cross validated with calorimetric detection using appropriate enzymatic substrate (TMB) and through SEM imaging. Current study indicates the potential of a bFBG sensor for rapid and real-time detection of bacteria and other specific bio-molecules. Future experiments will be aimed at packaging the sensor for on-site detection of clinically relevant analytes.

Acknowledgements The authors would like to thank the Advanced Facility for Microscopy and Microanalysis (AFMM) center, IISc, Bangalore for providing the facility for SEM imaging and Jayesh Adhikari for preparation of figures and graphical abstract. Dr. Sundarrajan Asokan thanks Robert Bosch Centre for Cyber Physical Systems (RBC-CPS), IISc, for partial support. Dr. Sai Siva Gorthi would like to acknowledge Department of Biotechnology's (DBT) IYBA for partial funding.

References

[1] P. I. Tarr, Clin. Infect. Dis. **20**(1), 1–8; quiz 9–10 (1995).
[2] P. S. Mead and P. M. Griffin, Lancet **352**(9135), 1207–1212 (1998).
[3] O. Savichtcheva and S. Okabe, Water Res. **40**(13), 2463–2476 (2006).
[4] V. P. Gannon, R. K. King, J. Y. Kim, and E. J. Thomas, Appl. Environ. Microbiol. **58**(12), 3809–3815 (1992).
[5] R. H. Yolken, H. B. Greenberg, M. H. Merson, R. B. Sack, and A. Z. Kapikian, J. Clin. Microbiol. **6**(5), 439–444 (1977).
[6] P. Arora, A. Sindhu, N. Dilbaghi, and A. Chaudhury, Biosens Bioelectron **28**(1), 1–12 (2011).
[7] A. Ahmed, J. V. Rushworth, N. A. Hirst, and P. A. Millner, Clin. Microbiol. Rev. **27**(3), 631–646 (2014).
[8] J. Andrade, R. Vanwagenen, D. Gregonis, K. Newby, and J. N. Lin, IEEE Trans Electron Devices **32**(7), 1175–1179 (1985).
[9] A. Leung, P. M. Shankar, and R. Mutharasan, Sens Actuators B Chem **125**(2), 688–703 (2007).
[10] X. Fan, I. M. White, S. I. Shopova, H. Zhu, J. D. Suter, and Y. Sun, Anal. Chim. Acta **620**(1–2), 8–26 (2008).
[11] A. Chryssis, S. Saini, S. Lee, H. Yi, W. E. Bentley, and M. Dagenais, IEEE J Sel Top Quantum Electron **11**(4), 864–872 (2005).
[12] M. P. DeLisa, Z. Zhang, M. Shiloach, S. Pilevar, C. C. Davis, J. S. Sirkis, and W. E. Bentley, Anal. Chem. **72**(13), 2895–2900 (2000).

[13] S. Maguis, G. Laffont, P. Ferdinand, B. Carbonnier, K. Kham, T. Mekhalif, and M. C. Millot, Opt Express **16**(23), 19049–19062 (2008).
[14] F. Baldini, M. Brenci, F. Chiavaioli, A. Giannetti, and C. Trono, Anal Bioanal Chem **402**(1), 109–116 (2011).
[15] M. Smietana, W. J. Bock, P. Mikulic, A. Ng, R. Chinnappan, and M. Zourob, Opt Express **19**(9), 7971–7978 (2011).
[16] S. M. Tripathi, W. J. Bock, P. Mikulic, R. Chinnappan, A. Ng, M. Tolba, and M. Zourob, Biosens Bioelectron **35**(1), 308–312 (2012).
[17] E. Brzozowska, M. Åšmietana, M. Koba, S. Grska, K. Pawlik, A. Gamian, and W. J. Bock, Biosens Bioelectron **67**(May), 93–99 (2015).
[18] N. D. Rees, S. W. James, R. P. Tatam, and G. J. Ashwell, Opt Lett **27**(9), 686–688 (2002).
[19] W. W. Morey, G. Meltz, and W. H. Glenn, Proc. SPIE **1169**, 98–107 (1990).
[20] K. O. Hill and G. Meltz, J Lightwave Technol **15**(8), 1263–1276 (1997).
[21] A. Kersey, M. Davis, H. Patrick, M. Leblanc, K. Koo, C. Askins, M. Putnam, and E. Friebele, J Lightwave Technol **15**(8), 1442–1463 (1997).
[22] A. Othonos, Rev Sci Instrum **68**(12), 4309–4341 (1997).
[23] R. Kashyap, Fiber Bragg Gratings (Academic Press, 1999).
[24] S. Melle, A. Alavie, S. Karr, T. Coroy, K. Liu, and R. Measures, IEEE Photonics Technol Lett **5**(2), 263–266 (1993).
[25] K. O. Hill, B. Malo, F. Bilodeau, D. C. Johnson, and J. Albert, Appl Phys Lett **62**(10), 1035–1037 (1993).
[26] D. Anderson, V. Mizrahi, T. Erdogan, and A. White, Electron. Lett. **29**(6), 566–568 (1993).
[27] G. T. Hermanson, Bioconjugate Techniques (Academic Press, July 2013).